

---

# DiffuMask-Editor: A Novel Paradigm of Integration Between the Segmentation Diffusion Model and Image Editing to Improve Segmentation Ability

---

Bo Gao

School of Intelligent Systems Engineering  
Sun Yat-sen University

Fangxu Xing

Department of Radiology  
Harvard Medical School

Daniel Tang\*

Interdisciplinary Security and Trust Centre (SnT)  
University of Luxembourg

## Abstract

Semantic segmentation models, like mask2former, often demand a substantial amount of manually annotated data, which is time-consuming and inefficient to acquire. Leveraging state-of-the-art text-to-image models like Midjourney and Stable Diffusion has emerged as an effective strategy for automatically generating synthetic data instead of human annotations. However, prior approaches have been constrained to synthesizing single-instance images due to the instability inherent in generating multiple instances with Stable Diffusion. To expand the domains and diversity of synthetic datasets, this paper introduces a novel paradigm named **DiffuMask-Editor**, which combines the Diffusion Model for Segmentation with Image Editing. By integrating multiple objects into images using Text2Image models, our method facilitates the creation of more realistic datasets that closely resemble open-world settings while simultaneously generating accurate masks. Our approach significantly reduces the laborious effort associated with manual annotation while ensuring precise mask generation. Experimental results demonstrate that synthetic data generated by **DiffuMask-Editor** enable segmentation methods to achieve superior performance compared to real data. Particularly in zero-shot backgrounds, **DiffuMask-Editor** achieves new state-of-the-art results on Unseen classes of VOC 2012. The code and models will be publicly available soon.

## 1 Introduction

Semantic segmentation [1, 2] is a critical computer vision component with profound implications across diverse applications. It is the cornerstone for achieving nuanced scene understanding, enabling advancements in autonomous driving, intelligent surveillance, and robotic navigation by deciphering intricate visual environments. Additionally, the precision of semantic segmentation significantly enhances object recognition and localization, thereby improving tasks like image retrieval and object identification. However, existing semantic segmentation models largely depend on robust, manually annotated data, which can be prohibitively expensive. For example, precise pixel-level annotations are required in medical imaging to delineate the boundaries of organs and structures, demanding expertise and meticulous attention.

To address this issue, some previous works have shifted focus to weak supervision, which involves training models with a smaller scale of data, such as image-level labels [3–7] and bounding boxes [8].

---

\*Corresponding author

This approach aims to balance annotation costs with testing performance. Unfortunately, it still suffers from drawbacks such as low accuracy and complex training strategies.

An alternative method involves synthesizing unrealistic datasets with pixel-wise labels. Previous researches [9–11], primarily based on Generative Adversarial Networks (GANs), have aimed to generate synthetic data to support supervised learning, thus reducing the need for extensive human annotation. However, due to the inherent limitations of GANs, such as heavy reliance on hyper-parameters and difficulties in capturing complex open-world correspondences between semantic information and objectives, these methods still face issues with accuracy and stability during training.

With the advancement of image generation technologies, diffusion models [12–14] have garnered considerable attention in the content generation community due to their stability and fidelity. Building on this technology, recent works such as DiffuMask [15] and DiffusionSeg [16] have successfully generated pairs of synthetic images and corresponding segmentation masks. DiffuMask [15] effectively uses intuitive textual prompts like ‘a photograph depicting a [class label]’ to generate image-mask pairs. Conversely, DiffusionSeg [16] specializes in generating synthetic datasets tailored for object discovery, which involves identifying prominent objects within an image. While these methods are limited to generating a single object segmentation mask per image, Dataset Diffusion [17] has been used to produce multiple objects along with precise segmentation masks. However, the accuracy of these masks can be significantly affected by occlusion between different objects.

Based on the description provided, we introduce **DiffuMask-Editor**, a novel module for generating synthetic images and masks. Unlike previous work, such as DiffuMask [15], this module can simultaneously generate multiple objects and their corresponding masks in a single image. The method utilizes the advanced text-to-image diffusion model, Stable Diffusion [18], which is trained on large-scale web datasets. As a zero-shot pre-trained model, it enables the generation of any type of picture without the constraints of closely related training sets, which will provide extremely rich data for segmentation models to improve performance. Building on DiffuMask [15], our core lies in how we add multiple objects to a single-instance image. To this end, we creatively combine semantic segmentation and image editing, driven by artificially imposed regulations that allow for accurate mask annotations. Specifically, we introduce three techniques: Adaptive Matching Thesaurus, which helps us select the most coherent and logical objects to add; Foreground Object Location, which identifies the precise location for the placement of objects chosen by the Adaptive Matching Thesaurus; and Image Harmonization, which integrates foreground objects seamlessly with the background. These synthetic data can then be utilized to train any semantic segmentation methods, such as mask2former [19], replacing real data and thus enhancing their robustness.

In summary, the main contributions of our work are as follows:

- We reverse the traditional segmentation task from image to mask to a process that starts with precise masks and then generates images when synthesizing segmentation datasets. This approach not only simplifies the acquisition of accurate masks for segmentation tasks but also enriches the data domain and enhances performance in open-world scenarios by adding foreground objects.
- We introduce the novel Adaptive Matching Thesaurus to determine and filter which types of objects can and cannot be added to the generated images by the diffusion model. We also introduce the Foreground Object Location to select appropriate locations, leveraging search-derived valid positions for mask annotation, and apply Image Harmonization to enhance the realism of synthetic images.
- We present the DiffuMask-Editor framework, capable of generating multiple objects in one image along with their accurate masks. To the best of our knowledge, this is the first work to innovatively collaborate on the diffusion model for segmentation and image editing. We have conducted extensive experiments and achieved promising performance gains on two large-scale datasets and open-world scenes.

## 2 Related Work

### 2.1 Text-to-image Diffusion Models

Text-to-image diffusion models have become a significant trend in image generation. Following the publication of "Diffusion Models Beat GANs on Image Synthesis" [20], an increasing number of diffusion model variants have emerged, with applications spanning image editing, image super-resolution, and more. For instance, Imagic [13] introduces a text-to-image diffusion model that aligns a text embedding with both the input image and target text, then fine-tunes the model to capture image-specific appearances for image editing purposes. IDM [14] proposes a denoising diffusion model with an implicit neural representation featuring a scale-controllable conditioning mechanism to address common issues such as over-smoothing and artifacts in continuous image super-resolution. According to DiffuMask [15], attention maps can be used as mask annotations roughly since the cross-attention layer is the only way through which text during the diffusion process can influence the image denoising, thus the images in the attention layer will exhibit 'attention' towards the objects described in the text.

### 2.2 Strongly and Weakly Supervised Semantic Segmentation

Due to the time-consuming and labor-intensive nature of strong supervision involving manual annotation, many researchers have shifted focus toward weakly supervised training approaches. These methods do not rely on pixel-wise labels but use simpler annotations such as points, bounding boxes [8], and image classification tasks [3–7], but they also provide the lowest precision. On the other hand, bounding boxes offer more effective results than fully supervised training, though they still require significant annotation. Another limitation of these approaches is their confinement to closed-set object categories. To overcome these challenges, models like DiffuMask [15], DiffusionSeg [16], ODISE [21], DiffSegmenter [22], and DifFSS [23] leverage powerful diffusion models in weakly-supervised semantic segmentation. They utilize attention maps within text-conditional diffusion models to generate rich data in image-mask pairs. These methods achieve promising results efficiently and effectively by correlating text prompts with foreground objects.

## 3 Methodology

In this paper, we explore the integration of semantic segmentation and image editing using existing pretrained diffusion models. We efficiently train existing segmentation modules using images that are first generated and then edited, along with their precise masks, and finally applied in open-world scenarios.

In generating datasets, the key shift in our approach is from acquiring precise masks to editing images, facilitated by a precise and imposed locating manner for mask annotation. In an open world with numerous objects, we face three primary challenges. First, it is essential to determine which objects can be appropriately added to generated images. For example, in an image of an airport produced by a diffusion model, it is logical to add airplanes but not giraffes. Second, it is crucial to decide where these objects should be placed within the image to ensure they fit the scene appropriately. For instance, a tree should be rooted on the ground rather than appearing to float in the air. Third, we must address discrepancies in physical conditions, such as lighting differences between the foreground objects and the background, to enhance the overall harmony.

To address these challenges, we propose a two-step strategy. Initially, we produce images with a single object per image and their corresponding masks, similar to the approaches used by DiffuMask [15] and DiffusionSeg [16] (Sec. 3.1). Subsequently, we proceed to the second phase of image editing to tackle the aforementioned issues (Sec. 3.2).

### 3.1 Single-object and Mask Generation

#### 3.1.1 Cross Attention Map in the Diffusion Model

Text-to-Image models (e.g., Stable Diffusion [18], Imagen [24], DALLE-2 [12]) are conditional diffusion models, with text prompt  $C_{text}$  to guide and influence the denoising process from the input, a Gaussian noise  $z_t$  to the latent image  $z_0$ . Specifically, Stable Diffusion consists of a text encoder  $\varsigma_\theta$ ,

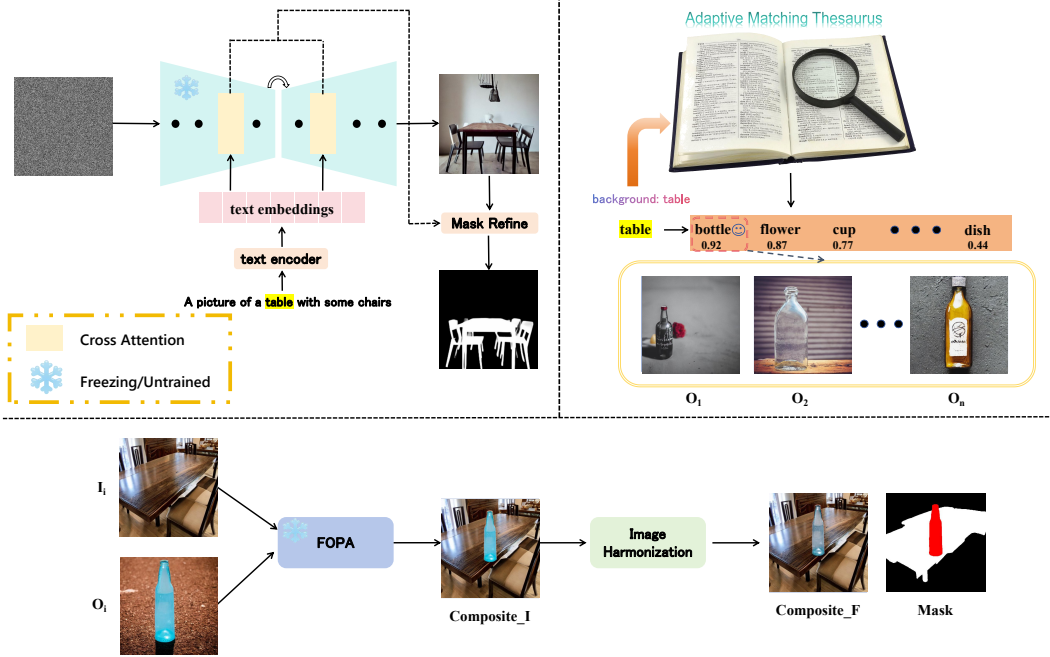


Figure 1: **The overall pipeline of DiffuMask-Editor.**  $I_i$  reflects the  $i_{th}$  background along with single-object by the same text prompt.  $O\{1, 2, \dots, n\}$  is the set of images of the object selected from our 'Thesaurus,' and  $O_i$  is the  $I_{th}$  object-image.  $Composite\_I$  denotes the initial image after the Object Location, while  $Composite\_F$  is the final image after Image Harmonization along with mask annotation  $Mask$ .

a variational auto-encoder (VAE), and a conditional UNet  $\epsilon_\theta$ . During the progress, the text prompt  $C_{text}$  is input into the cross-attention layers to be fused with the visual latent embeddings. This advanced fusion mode allows us to use the cross-attention map to help the model concentrate on the objects referred to in the texts. For a given step  $t$ , assuming  $z_t \in \mathbb{R}^{H \times W \times C}$ , where  $H$  is the height,  $W$  is the width, and  $C$  reflects the number of channels, it is linearly projected into the Query matrix  $Q = ZW_q$ . The text prompt  $C_{text}$  is processed by the text encoder  $s_\theta$ , producing the text embeddings  $X = s_\theta(C_{text}) \in \mathbb{R}^{L \times d}$ , which are linearly transformed into a Key matrix  $K = XW_k$  and Value matrix  $V = XW_v$ . Here,  $W_q$ ,  $W_k$ , and  $W_v$  are linear transformations applied to the input features to obtain the query, key, and value. The cross attention map at the step  $t$  and the  $n_{th}$  layer of UNet is calculated by the below formula:

$$\mathcal{M}_C^{n,t} = \text{Softmax} \left( \frac{QK^T}{\sqrt{d}} \right), \quad (1)$$

where  $\mathcal{M}_C^{n,t} \in \mathbb{R}^{H \times W \times L}$  after projection and  $d$  reflects the features' dimension.

### 3.1.2 Mask Generation and Refinement

Observations from [17] indicate that using different ranges of timesteps only marginally affects the final result. Therefore, averaging these cross-attention maps over layers and timesteps is a practical method for achieving feature fusion, applied to four different resolutions:  $8 \times 8$ ,  $16 \times 16$ ,  $32 \times 32$ , and  $64 \times 64$  assuming the input size (width, height) is  $(512, 512)$ .

$$\mathcal{M}_C = \frac{1}{N \times T} \sum_{n=1}^N \sum_{t=0}^T \mathcal{M}_C^{n,t}, \quad (2)$$

Although the cross-attention maps  $\mathcal{M}_C$  provide an indication of the location of the target classes in the image, they still appear vague and inaccurate. Following the approach of DiffuMask [15], which associates different classes of objects with different segmentation thresholds, we refine the vague masks. By utilizing AffinityNet [3], which helps identify object boundaries or perform pixel-level

classification by learning the relationships or similarities between different regions in an image, we can generate multiple masks for foreground images of different classes based on varying thresholds. By comparing the intersection over union (IOU) with the output of AffinityNet [3]’s output, we can select the segmentation image that corresponds to the highest IOU value, thus obtaining the optimal segmentation image for the selected threshold.

### 3.2 Image Editing

By innovatively transforming segmentation tasks into image editing tasks, precise segmentation masks for foreground objects can be easily obtained through the second step of localization. Firstly, we construct an adaptive matching lexicon by leveraging the vast array of terms in text-image pairs found on the internet, aiming to collect foreground objects that semantically fit the background. Secondly, we employ a novel discriminative network to localize the selected objects, thereby ensuring their geometric coherence. Lastly, we achieve harmonization between foreground and background tasks in terms of physics through image harmonization. Sec. 3.2.1 will introduce how to construct a matching lexicon to select semantically appropriate foreground objects. Sec. 3.2.2 will discuss the application of a fast discriminative network for foreground object localization and dimension standardization. Sec. 3.2.3 will explain the final step of image harmonization, aiming to normalize and unify the physical conditions, such as the lighting of foreground objects with the background.

#### 3.2.1 Adaptive Matching Thesaurus

The training process of Stable Diffusion [18] leverages the extensive LAION dataset [25], which provides a rich array of text-image pairs and deriving semantic alignment between foreground objects and backgrounds directly from image feature analysis can be overly complex and may lead to overfitting in network design. Therefore, beginning with text-based analysis is deemed more reasonable and efficient. In this paper, we construct a comprehensive matching lexicon to establish correspondences in an open-world scenario, measuring the semantic similarity between foreground objects and backgrounds from a language understanding perspective. To quantitatively assess this matching, we calculate probability values based on the occurrence positions and frequencies of foreground object terms within a large text-image-pair database. These probabilities serve as a measure of similarity. The following formula is used to calculate the semantic similarity between object  $i$  and background  $j$ :

$$\text{Similarity } < o_i, b_j > = \frac{\sum_{\text{text}_{b_j} \in \text{Texts}_{b_j}} \mathbb{I}(o_i \in \text{text}_{B_j})}{\sum_{\text{text}_{b_j} \in \text{Texts}_{B_j}} \text{text}_{b_j}} \quad (3)$$

where  $\text{Texts}_{b_j}$  represents the set of all text prompts containing the background  $b_j$ , and  $\text{text}_{b_j}$  denotes each element within this set..

Using this formula, we can establish a semantic summary table for foreground and background, as shown in 2, thus enabling the collection of appropriate object classes for embedding.

#### 3.2.2 Foreground Object Location

Due to the fast speed, efficiency, and time-saving characteristics, the Fast Object Placement Assessment (FOPA) [26] directly generates a heatmap to identify the optimal position, using the foreground target image, its segmentation binary mask, and the background image as inputs. The goal of this model is to evaluate all positions in a single pass, akin to pixel-level classification tasks in semantic segmentation. FOPA [26] utilizes a U-Net-like [27] structure (Encoder and Decoder) to encode the features of foreground targets and backgrounds. As the SOPA model [28] has already demonstrated the capability to learn background and foreground features, it directly utilizes the SOPA decoder within the FOPA model’s architecture, as mentioned in the "Background Prior Transfer" section. Additionally, following the feature loss approach introduced in literature [29, 30], FOPA [26] leverages each pixel-wise output feature to mimic the image-level features of corresponding composite images from the SOPA model [28], where each pixel on the output feature map corresponds to a composite image obtained by pasting the foreground at this location.

After this stage, we generate heatmaps of newly added objects. To determine the final location (accurate masks), we also need to identify the center point of the heatmap as our objects’ center

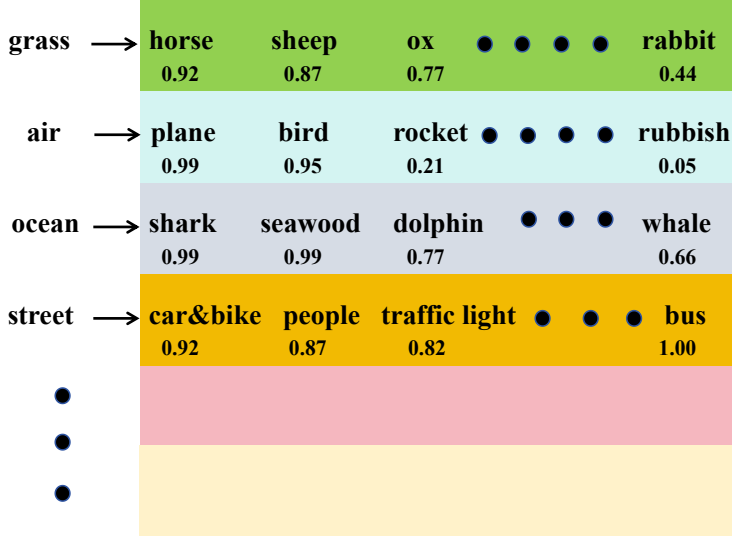


Figure 2: The thesaurus is based on the multiple text-image pairs.

point. Consequently, by fixing the center point and using the scale between the object image and the background image, we can determine the appropriate size of the added objects, thereby facilitating the creation of the bounding box  $[x, y, w, h]$  that locates the new objects.

$$\begin{aligned} center_x &= \underset{(x,y)}{\operatorname{argmax}} F_h(x, y), \quad w = center_x - \gamma_w * w_o / 2 \\ center_y &= \underset{(x,y)}{\operatorname{argmax}} F_h(x, y), \quad h = center_y - \gamma_h * h_o / 2 \end{aligned} \quad (4)$$

where  $F_h(x, y)$  indicating the heatmap,  $\gamma_w$  and  $\gamma_h$  respectively representing the scale of width and height,  $w_o$  and  $h_o$  respectively noting the width and height of object image.

### 3.2.3 Image Harmonization

Image harmonization is more like a style transfer task, but how to choose the normalization layer in the model is a question worth considering. There are several normalization methods, such as Batch Normalization(BN) [31], Layer Normalization(LN) [32], Instance Normalization (IN) [33], and Group Normalization(GN) [34]. The Batch Normalization (BN) [31] or Instance Normalization (IN) [32], using the same mean and variance as those of the background features, results in the background features being influenced by statistics from the foreground, thereby limiting the ability to learn style consistency in subsequent layers. Layer Normalization (LN) [32] and Group Normalization (GN) [34], based on channel-wise normalization, can significantly disrupt the features of each channel, thus undermining the effective transfer of the background features to the foreground objects.

Therefore, we adopt RAIN [35] as our starting point and utilize the efficient and effective AdaIn plugin for our image harmonization component. The new plugin avoids the shortcomings of the normalization methods mentioned above by separately extracting features from the background and foreground objects, which exclusively transfers statistics from background features to normalized foreground features, independent of the inconsistent foreground objects. Through the combination of the UNet-decoder and AdaIn plugin, we could gain the harmonious images as displayed in 1.

## 4 Experiments and Analysis

### 4.1 Datasets and Metrics

**PASCAL-VOC2012** [36] The VOC2012 dataset comprises hundreds of images annotated with bounding boxes and pixel-wise segmentation masks for 20 object classes, facilitating tasks like object

detection and semantic segmentation. It includes common categories such as person, dog, cat, car, and bicycle, with a balanced training/validation split for effective model training and evaluation.

**Cityscapes** [37] Cityscapes, a semantic understanding image dataset focused on urban street scenes, primarily consists of high-quality pixel-level annotated images capturing driving scenarios in urban environments from 50 different cities, with 2975 for training, 500 for validation, and 1525 for testing, totaling 5000 images across 19 classes. Furthermore, it includes 20,000 roughly annotated images (gt coarse).

**Metrics** The mean intersection-over-union (**mIoU**) is a widely adopted metric for evaluating semantic segmentation performance, as utilized in this context [36, 19]. To assess open-vocabulary segmentation, akin to previous studies [38, 39], the mIoU is computed over seen classes, unseen classes, and their harmonic mean is employed.

## 4.2 Implementation Details

**Synthetic data for training.** We follow the details from DiffuMask [15]. Specifically, for Pascal-VOC 2012 [36], we augment  $10k$  images per category and filter out  $7k$  images. Consequently, we assemble a final training set of  $60k$  synthetic images across 20 classes, all with a spatial resolution of  $512 \times 512$  pixels. Regarding Cityscapes [40], we focus on evaluating two significant classes, namely 'Human' and 'Vehicle,' encompassing six sub-classes: person, rider, car, bus, truck, and train. We generate  $30k$  images for each sub-category, with a final selection of  $10k$  images per class.

**The basic tools.** We leverage foundational components such as pre-trained Stable Diffusion [18], the text encoder from CLIP [41], object placement from FOPA [26], and image harmonization techniques [35] as foundational components. And we utilize Mask2Former [19] as the baseline model for dataset evaluation. Without finetuning Stable Diffusion or training any module for individual categories, we maintain parameter optimization and settings consistent with the original papers, including initialization, data augmentation, batch size, and learning rate. All experiments are conducted using 8 Tesla A100 GPUs.

## 4.3 Comparison with State-of-the-art Methods

Table 1: **Result of Semantic Segmentation on the VOC 2012 val.** And  $mIoU$  is for 20 classes. 'S' and 'R' refer to 'Synthetic' and 'Real'.

Train Set	Number	Backbone	Semantic Segmentation (IoU) for Selected Classes/%												mIoU	
			aeroplane	bird	boat	bus	car	cat	chair	cow	dog	horse	person	sheep		
<i>Train with Pure Real Data</i>																
VOC	R: 10.6k (all)	R50	87.5	94.4	70.6	95.5	87.7	92.2	44.0	85.4	89.1	82.1	89.2	80.6	53.6	77.3
	R: 10.6k (all)	Swin-B	97.0	93.7	71.5	91.7	89.6	96.5	57.5	95.9	96.8	94.4	92.5	95.1	65.6	84.3
	R: 5.0k	Swin-B	95.5	87.7	77.1	96.1	91.2	95.2	47.3	90.3	92.8	94.6	90.9	93.7	61.4	83.4
<i>Train with Pure Synthetic Data</i>																
DiffuMask	S: 60.0k	R50	80.7	86.7	56.9	81.2	74.2	79.3	14.7	63.4	65.1	64.6	71.0	64.7	27.8	57.4
	S: 60.0k	Swin-B	90.8	92.9	67.4	88.3	82.9	92.5	27.2	92.2	86.0	89.0	76.5	92.2	49.8	70.6
ours	S: 60.0k	R50	82.1	88.3	58.3	83.1	79.0	81.6	17.7	65.4	67.3	65.9	75.0	66.0	29.6	62.5
	S: 60.0k	Swin-B	92.1	94.7	69.2	88.2	84.1	92.4	30.4	92.7	87.4	89.1	78.8	92.2	52.0	72.0
<i>Finetune on Real Data</i>																
DiffuMask	S: 60.0k + R: 5.0k	R50	85.4	92.8	74.1	92.9	83.7	91.7	38.4	86.5	86.2	82.5	87.5	81.2	39.8	77.6
	S: 60.0k + R: 5.0k	Swin-B	95.6	94.4	72.3	96.9	92.9	96.6	51.5	96.7	95.5	96.1	91.5	96.4	70.2	84.9
ours	S: 60.0k + R: 5.0k	R50	86.5	94.1	73.7	94.3	85.7	91.9	41.3	87.2	89.6	83.0	88.0	80.6	46.8	78.9
	S: 60.0k + R: 5.0k	Swin-B	96.2	94.8	73.5	96.9	93.9	96.7	52.3	96.9	95.7	97.2	92.1	96.5	71.1	85.6

### 4.3.1 Semantic Segmentation

For the **VOC2012 dataset** [36], as shown in Table 1, our model outperforms the competition in nearly all of the 20 classes. Compared to DiffuMask [15], when trained with purely synthetic data, our DiffuMask-Editor enhances the mIoU by nearly 8% (from 57.4% to 62.5%) using Resnet50 [42] and from 70.6% to 72.0% using Swin-B [42]. In the "Finetune on Real Data" segment, which combines 60,000 synthetic images with 5,000 real images, the mIoU also increases by 9%. Most notably, for categories such as "bird," "boat," "cat," "chair," and "sofa," our model demonstrates exceptionally strong performance, exceeding that achieved through training on real data by a significant margin, with an average gap exceeding 2%.

Regarding the **Cityscapes dataset** [40], our model continues to show robust capabilities. Compared to DiffuMask [15], we have significantly reduced the performance gap with training on actual data, decreasing the difference from 10% to single digits. Moreover, relying solely on generated data, we have improved our previous method from 70% to over 80%, surpassing the 80% mark.

Table 2: **The mIoU (%) of Semantic Segmentation on Cityscapes val.** ‘Human’ includes two sub-classes person and rider. ‘Vehicle’ includes four sub-classes, *i.e.* car, bus, truck, and train. Mask2former [19] with ResNet50 is used.

Train Set	Number	Backbone	Category/%		mIoU
			Human	Vehicle	
<i>Train with Pure Real Data</i>					
Cityscapes	3.0k (all)	R50	83.4	94.5	89.0
	3.0k (all)	Swin-B	85.5	96.0	90.8
	1.5k	Swin-B	84.6	95.3	90.0
<i>Train with Pure Synthetic Data</i>					
DiffuMask	100.0k	R50	70.7	85.3	78.0
DiffuMask	100.0k	Swin-B	72.1	87.0	79.6
ours	100.0k	R50	73.9	86.7	82.1
ours	100.0k	Swin-B	75.7	90.4	83.5

Table 3: **Performance for Zero-Shot Semantic Segmentation Task on PASCAL VOC.** ‘Seen,’ ‘Unseen,’ and ‘Harmonic’ denote mIoU of seen, unseen categories, and their harmonic mean. Priors are trained with real data and masks.

Methods	Train Set/%		mIoU/%		
	Type	Categories	Seen	Unseen	Harmonic
<i>Manual Mask Supervision</i>					
ZS3 [43]	real	15	78.0	21.2	33.3
CaGNet [44]	real	15	78.6	30.3	43.7
Joint [45]	real	15	77.7	32.5	45.9
STRICT [46]	real	15	82.7	35.6	49.8
SIGN [39]	real	15	83.5	41.3	55.3
ZegFormer [38]	real	15	86.4	63.6	73.3
<i>Pseudo Mask Supervision from Model pre-trained on COCO [47]</i>					
Li <i>et al.</i> [48] (ResNet101)	synthetic	15+5	62.8	50.0	55.7
<i>Text(Prompt) Supervision</i>					
DiffuMask (ResNet50)	synthetic	15+5	60.8	50.4	55.1
DiffuMask (ResNet101)	synthetic	15+5	62.1	50.5	55.7
DiffuMask (Swin-B)	synthetic	15+5	71.4	65.0	68.1
ours (ResNet50)	synthetic	15+5	63.9	57.0	61.6
ours (ResNet101)	synthetic	15+5	65.2	57.5	62.6
ours (Swin-B)	synthetic	15+5	74.0	<b>66.6</b>	71.5

#### 4.3.2 Zero-Shot Segmentation

Despite our model not being fine-tuned, it retains the capability for open-world segmentation. As indicated in Table 3, compared to many previous methods trained exclusively on real images and manually annotated masks, it achieves state-of-the-art results in zero-shot scenarios. All data automatically generated by DiffuMask-Editor are synthetic, eliminating the laborious manual annotation and dataset construction processes. We have also expanded the scope from single objects to multiple instances, enriching the dataset without introducing significant additional effort. Even when using the COCO dataset [47] to predict pseudo labels, which incurs higher computational costs, our approach, relying only on synthetic data, achieves a promising result of 66.6% on unseen classes, representing an almost 3% improvement over previous methods. More visualization results are in (A).

#### 4.4 Ablation Study

**Role of Mask Refinement** Table 4 displays that there is a 3% gap between ‘without Mask Refinement’ and our method. It means that at the first stage, the cross-attention maps are so vague and inaccurate that the noisy data could influence the performance and robustness of the segmentation models.

Table 4: **Ablation Study.** The outcomes are shown on the VOC 2012 validation dataset under the condition of finetuning on real data, with the average  $mIoU(\%)$  of all classes.

Methods	$mIoU$
All	78.9
without Mask Refinement	75.4
without Adaptive Matching Thesaurus	76.3
without Foreground Object Location	77.1
without Image Harmonization	78.0

**Role of Adaptive Matching Thesaurus** As discussed in Section 3.2.1, the thesaurus plays a vital role in filtering unfit objects semantically. As shown in Table 4, a 2.6% gap can be witnessed for all classes on average. This gap is the corroboration to justify the essence of semantic coherence in the field of semantic segmentation.

**Effectiveness of Foreground Object Location** Without ‘Foreground Object Location’, we could not get nearly realistic images. Even in a simple photo of two airplanes in the sky, if there isn’t an appropriate positioning, the airplanes might overlap. Such dirty data can significantly interfere with the training of segmentation models and affect their performance. Thus, there is a 1.8% gap.

**Effectiveness of Image Harmonization** Since image harmonization is a specific task studied in computer vision, it naturally becomes a very important factor. Without ‘Image Harmonization’, the intact pipeline lags behind our method by close to 1% demonstrated in Table 4.

## 4.5 Analysis

### 4.5.1 Why DiffuMask-Editor is superior to DiffuMask?

In our experiments, we recognize the limitations of Stable Diffusion in generating multiple instances, as previously demonstrated in multi-category generation [48]. Therefore, DiffuMask [15] is intentionally limited to single foreground objects, potentially introducing dataset bias. In real-world scenarios, backgrounds rarely consist of solitary objects. Thus, the dataset curated by DiffuMask [15] may predispose models to such scenarios, complicating performance evaluation on diverse datasets. Furthermore, our proposed **DiffuMask-Editor** serves as a data augmentation technique that not only enriches the dataset but also broadens its scope, thereby enhancing the segmentation model’s learning capabilities, especially in real-world scenarios. Moreover, by transforming the task of obtaining precise masks into an image editing task, we can effortlessly obtain mask annotations simultaneously while localizing the targets. Since we specify the positions ourselves through the model, it is straightforward to have accurate mask annotations. Compared to the traditional approach of deriving masks from images, our reverse thinking easily addresses the issue of inaccurate masks, and precise masks will naturally significantly improve the performance of segmentation models.

### 4.5.2 Bridge the gap between the close-set and open-world.

As illustrated in Table 3, we thoroughly examined the model’s performance in real-world scenarios. Our model exhibits state-of-the-art performance across previously unseen categories, thus affirming its dominance in the realm of open-world data analysis. Further analysis revealed that the model’s exceptional ability to handle zero-shot scenarios stems not only from its architectural design but also from the diversity and richness of the training data. Unlike earlier approaches that struggled with data scarcity and domain-specific biases, we proactively enhanced our training dataset with a broad array of foreground objects from diverse domains. This strategic enhancement not only expands the model’s exposure to a variety of visual stimuli but also ensures the seamless integration of new, unseen elements into its predictive framework.

## 5 Conclusion

This paper introduces a novel approach for generating segmentation masks by integrating semantic segmentation with image editing, thereby eliminating the need for manual annotation through the use of powerful generative models. Distinct from previous methods, our model is capable of

simultaneously generating images with multiple instances, enhancing its adaptability to real-world conditions. Specifically, the combination of single-instance and multiple-instance images within a dataset significantly boosts the performance of segmentation models. This advancement enables our model, named **DiffuMask-Editor**, to excel in scenarios involving open-world segmentation. Looking forward, we plan to directly extract multi-instance, multi-object segmentation masks from the Diffusion Model to facilitate comprehensive end-to-end dataset augmentation.

## References

- [1] Jonathan Long, Evan Shelhamer, and Trevor Darrell. Fully convolutional networks for semantic segmentation. In *Proc. IEEE Conf. Comp. Vis. Patt. Recogn.*, pages 3431–3440, 2015.
- [2] Yawei Luo, Liang Zheng, Tao Guan, Junqing Yu, and Yi Yang. Taking a closer look at domain shift: Category-level adversaries for semantics consistent domain adaptation. In *Proceedings of the IEEE/CVF conference on computer vision and pattern recognition*, pages 2507–2516, 2019.
- [3] Jiwoon Ahn and Suha Kwak. Learning pixel-level semantic affinity with image-level supervision for weakly supervised semantic segmentation. In *Proceedings of the IEEE conference on computer vision and pattern recognition*, pages 4981–4990, 2018.
- [4] Jungbeom Lee, Eunji Kim, and Sungroh Yoon. Anti-adversarially manipulated attributions for weakly and semi-supervised semantic segmentation. In *Proceedings of the IEEE/CVF Conference on Computer Vision and Pattern Recognition*, pages 4071–4080, 2021.
- [5] Tong Wu, Junshi Huang, Guangyu Gao, Xiaoming Wei, Xiaolin Wei, Xuan Luo, and Chi Harold Liu. Embedded discriminative attention mechanism for weakly supervised semantic segmentation. In *Proceedings of the IEEE/CVF Conference on Computer Vision and Pattern Recognition*, pages 16765–16774, 2021.
- [6] Lian Xu, Wanli Ouyang, Mohammed Bennamoun, Farid Boussaid, Ferdous Sohel, and Dan Xu. Leveraging auxiliary tasks with affinity learning for weakly supervised semantic segmentation. In *Proceedings of the IEEE/CVF International Conference on Computer Vision*, pages 6984–6993, 2021.
- [7] Lixiang Ru, Yibing Zhan, Baosheng Yu, and Bo Du. Learning affinity from attention: End-to-end weakly-supervised semantic segmentation with transformers. In *Proceedings of the IEEE/CVF Conference on Computer Vision and Pattern Recognition*, pages 16846–16855, 2022.
- [8] Jungbeom Lee, Jihun Yi, Chaehun Shin, and Sungroh Yoon. Bbam: Bounding box attribution map for weakly supervised semantic and instance segmentation. In *Proceedings of the IEEE/CVF conference on computer vision and pattern recognition*, pages 2643–2652, 2021.
- [9] Yuxuan Zhang, Huan Ling, Jun Gao, Kangxue Yin, Jean-Francois Lafleche, Adela Barriuso, Antonio Torralba, and Sanja Fidler. Datasetgan: Efficient labeled data factory with minimal human effort. In *Proceedings of the IEEE/CVF Conference on Computer Vision and Pattern Recognition*, pages 10145–10155, 2021.
- [10] Nontawat Tritrong, Pitchaporn Rewatbowornwong, and Supasorn Suwajanakorn. Repurposing gans for one-shot semantic part segmentation. In *Proceedings of the IEEE/CVF Conference on Computer Vision and Pattern Recognition (CVPR)*, pages 4475–4485, June 2021.
- [11] Daiqing Li, Huan Ling, Seung Wook Kim, Karsten Kreis, Sanja Fidler, and Antonio Torralba. Bigdatasetgan: Synthesizing imagenet with pixel-wise annotations. In *Proceedings of the IEEE/CVF Conference on Computer Vision and Pattern Recognition*, pages 21330–21340, 2022.
- [12] Aditya Ramesh, Prafulla Dhariwal, Alex Nichol, Casey Chu, and Mark Chen. Hierarchical text-conditional image generation with clip latents. *arXiv preprint arXiv:2204.06125*, 2022.
- [13] Bahjat Kawar, Shiran Zada, Oran Lang, Omer Tov, Huiwen Chang, Tali Dekel, Inbar Mosseri, and Michal Irani. Imagic: Text-based real image editing with diffusion models. In *Proceedings of the IEEE/CVF Conference on Computer Vision and Pattern Recognition*, pages 6007–6017, 2023.

[14] Sicheng Gao, Xuhui Liu, Bohan Zeng, Sheng Xu, Yanjing Li, Xiaoyan Luo, Jianzhuang Liu, Xiantong Zhen, and Baochang Zhang. Implicit diffusion models for continuous super-resolution. In *Proceedings of the IEEE/CVF Conference on Computer Vision and Pattern Recognition (CVPR)*, pages 10021–10030, June 2023.

[15] Weijia Wu, Yuzhong Zhao, Mike Zheng Shou, Hong Zhou, and Chunhua Shen. Diffumask: Synthesizing images with pixel-level annotations for semantic segmentation using diffusion models. *Proc. Int. Conf. Computer Vision (ICCV 2023)*, 2023.

[16] Chaofan Ma, Yuhuan Yang, Chen Ju, Fei Zhang, Jinxiang Liu, Yu Wang, Ya Zhang, and Yanfeng Wang. Diffusionseg: Adapting diffusion towards unsupervised object discovery, 2023.

[17] Quang Ho Nguyen, Truong Vu, Anh Tran, and Khoi Nguyen. Dataset diffusion: Diffusion-based synthetic dataset generation for pixel-level semantic segmentation. In *Thirty-Seventh Conference on Neural Information Processing Systems*, 2023.

[18] Robin Rombach, Andreas Blattmann, Dominik Lorenz, Patrick Esser, and Björn Ommer. High-resolution image synthesis with latent diffusion models. In *Proceedings of the IEEE/CVF Conference on Computer Vision and Pattern Recognition*, pages 10684–10695, 2022.

[19] Bowen Cheng, Ishan Misra, Alexander G Schwing, Alexander Kirillov, and Rohit Girdhar. Masked-attention mask transformer for universal image segmentation. In *Proceedings of the IEEE/CVF Conference on Computer Vision and Pattern Recognition*, pages 1290–1299, 2022.

[20] Prafulla Dhariwal and Alex Nichol. Diffusion models beat gans on image synthesis, 2021.

[21] Jiarui Xu, Sifei Liu, Arash Vahdat, Wonmin Byeon, Xiaolong Wang, and Shalini De Mello. Open-Vocabulary Panoptic Segmentation with Text-to-Image Diffusion Models. *arXiv preprint arXiv:2303.04803*, 2023.

[22] Jinglong Wang, Xiawei Li, Jing Zhang, Qingyuan Xu, Qin Zhou, Qian Yu, Lu Sheng, and Dong Xu. Diffusion model is secretly a training-free open vocabulary semantic segmenter, 2023.

[23] Weimin Tan, Siyuan Chen, and Bo Yan. Diffss: Diffusion model for few-shot semantic segmentation, 2023.

[24] Chitwan Saharia, William Chan, Saurabh Saxena, Lala Li, Jay Whang, Emily Denton, Seyed Kamyar Seyed Ghasemipour, Burcu Karagol Ayan, S. Sara Mahdavi, Rapha Gontijo Lopes, Tim Salimans, Jonathan Ho, David J Fleet, and Mohammad Norouzi. Photorealistic text-to-image diffusion models with deep language understanding, 2022.

[25] Christoph Schuhmann, Romain Beaumont, Richard Vencu, Cade Gordon, Ross Wightman, Mehdi Cherti, Theo Coombes, Aarush Katta, Clayton Mullis, Mitchell Wortsman, Patrick Schramowski, Srivatsa Kundurthy, Katherine Crowson, Ludwig Schmidt, Robert Kaczmarczyk, and Jenia Jitsev. Laion-5b: An open large-scale dataset for training next generation image-text models, 2022.

[26] Li Niu, Qingyang Liu, Zhenchen Liu, and Jiangtong Li. Fast object placement assessment, 2022.

[27] Olaf Ronneberger, Philipp Fischer, and Thomas Brox. U-net: Convolutional networks for biomedical image segmentation. In *Medical image computing and computer-assisted intervention–MICCAI 2015: 18th international conference, Munich, Germany, October 5-9, 2015, proceedings, part III 18*, pages 234–241. Springer, 2015.

[28] Liu Liu, Zhenchen Liu, Bo Zhang, Jiangtong Li, Li Niu, Qingyang Liu, and Liqing Zhang. Opa: Object placement assessment dataset. *arXiv preprint arXiv:2107.01889*, 2021.

[29] Quanquan Li, Shengying Jin, and Junjie Yan. Mimicking very efficient network for object detection. In *Proceedings of the ieee conference on computer vision and pattern recognition*, pages 6356–6364, 2017.

[30] Xiaochuan Wang, Aiguo Chen, Liang Zhang, Yi Gu, Mang Xu, and Haoyuan Yan. Distilling the knowledge of multiscale densely connected deep networks in mechanical intelligent diagnosis. *Wireless Communications and Mobile Computing*, 2021:1–12, 2021.

- [31] Sergey Ioffe and Christian Szegedy. Batch normalization: Accelerating deep network training by reducing internal covariate shift, 2015.
- [32] Jimmy Lei Ba, Jamie Ryan Kiros, and Geoffrey E. Hinton. Layer normalization, 2016.
- [33] Dmitry Ulyanov, Andrea Vedaldi, and Victor Lempitsky. Instance normalization: The missing ingredient for fast stylization, 2017.
- [34] Yuxin Wu and Kaiming He. Group normalization, 2018.
- [35] Jun Ling, Han Xue, Li Song, Rong Xie, and Xiao Gu. Region-aware adaptive instance normalization for image harmonization. In *Proceedings of the IEEE/CVF conference on computer vision and pattern recognition*, pages 9361–9370, 2021.
- [36] Mark Everingham, Luc Van Gool, Christopher KI Williams, John Winn, and Andrew Zisserman. The pascal visual object classes (voc) challenge. *International journal of computer vision*, 88(2):303–338, 2010.
- [37] Marius Cordts, Mohamed Omran, Sebastian Ramos, Timo Rehfeld, Markus Enzweiler, Rodrigo Benenson, Uwe Franke, Stefan Roth, and Bernt Schiele. The cityscapes dataset for semantic urban scene understanding. In *Proceedings of the IEEE conference on computer vision and pattern recognition*, pages 3213–3223, 2016.
- [38] Jian Ding, Nan Xue, Gui-Song Xia, and Dengxin Dai. Decoupling zero-shot semantic segmentation. In *Proc. CVPR*, 2022.
- [39] Jiaxin Cheng, Soumyaroop Nandi, Prem Natarajan, and Wael Abd-Almageed. Sign: Spatial-information incorporated generative network for generalized zero-shot semantic segmentation. In *Proc. ICCV*, 2021.
- [40] Marius Cordts, Mohamed Omran, Sebastian Ramos, Timo Rehfeld, Markus Enzweiler, Rodrigo Benenson, Uwe Franke, Stefan Roth, and Bernt Schiele. The cityscapes dataset for semantic urban scene understanding. In *Proceedings of the IEEE conference on computer vision and pattern recognition*, pages 3213–3223, 2016.
- [41] Alec Radford, Jong Wook Kim, Chris Hallacy, Aditya Ramesh, Gabriel Goh, Sandhini Agarwal, Girish Sastry, Amanda Askell, Pamela Mishkin, Jack Clark, et al. Learning transferable visual models from natural language supervision. In *International conference on machine learning*, pages 8748–8763. PMLR, 2021.
- [42] Kaiming He, Xiangyu Zhang, Shaoqing Ren, and Jian Sun. Deep residual learning for image recognition. In *Proceedings of the IEEE conference on computer vision and pattern recognition*, pages 770–778, 2016.
- [43] Maxime Bucher, Tuan-Hung Vu, Matthieu Cord, and Patrick Pérez. Zero-shot semantic segmentation. *NeurIPS*, 2019.
- [44] Zhangxuan Gu, Siyuan Zhou, Li Niu, Zihan Zhao, and Liqing Zhang. Context-aware feature generation for zero-shot semantic segmentation. In *ACM MM*, 2020.
- [45] Donghyeon Baek, Youngmin Oh, and Bumsub Ham. Exploiting a joint embedding space for generalized zero-shot semantic segmentation. In *Proc. ICCV*, 2021.
- [46] Giuseppe Pastore, Fabio Cermelli, Yongqin Xian, Massimiliano Mancini, Zeynep Akata, and Barbara Caputo. A closer look at self-training for zero-label semantic segmentation. In *Proc. CVPRW*, 2021.
- [47] Tsung-Yi Lin, Michael Maire, Serge Belongie, James Hays, Pietro Perona, Deva Ramanan, Piotr Dollár, and C Lawrence Zitnick. Microsoft coco: Common objects in context. In *Proc. ECCV*, 2014.
- [48] Ziyi Li, Qinye Zhou, Xiaoyun Zhang, Ya Zhang, Yanfeng Wang, and Weidi Xie. Guiding text-to-image diffusion model towards grounded generation. *arXiv preprint arXiv:2301.05221*, 2023.

## A Appendix / supplemental material

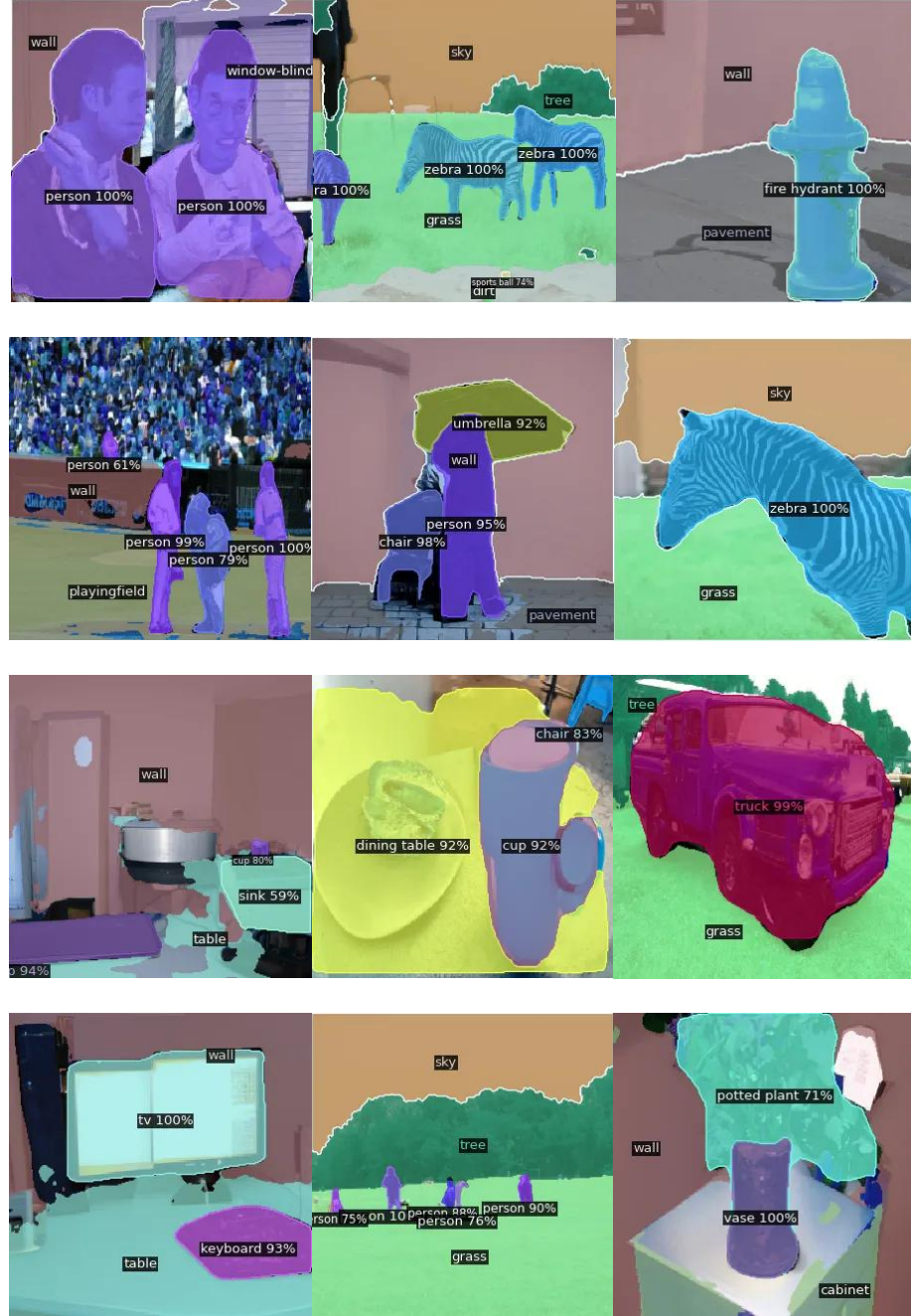


Figure 3: Display of generated images and masks.

Figure 3 shows generated images with boxes and masks. As is displayed, our method has achieved very promising results, generating very realistic images, while also having high-precision mask and box annotations. But when there is occlusion, there will still be the issue of inaccurate masks and a certain degree of impact on the quality of generated images.